Nuclear Engineering and Design 239 (2009) 1246–1253

Contents lists available at ScienceDirect

Nuclear Engineering and Design

journal homepage: www.elsevier.com/locate/nucengdes

Master Curve and Unified Curve applicability to highly neutron irradiated Western type reactor pressure vessel steels

Conrad Zurbuchen [a,*], Hans-Werner Viehrig [a,1], Frank-Peter Weiss [b,2]

[a] Department of Material and Component Safety, Institute of Safety Research, Research Centre Dresden-Rossendorf e.V., Institute of Safety Research, POB 510119, 01314 Dresden, Germany
[b] Institute of Safety Research, Research Centre Dresden-Rossendorf e.V., POB 510119, 01314 Dresden, Germany

ARTICLE INFO

Article history:
Received 6 March 2008
Received in revised form 2 March 2009
Accepted 10 March 2009

ABSTRACT

While the Master Curve (MC) method is gradually entering brittle fracture safety assessment procedures world-wide, knowledge is still lacking about its limits of applicability to highly neutron irradiated material. In this paper two reactor pressure vessel (RPV) steels A533B Cl.1 (IAEA reference material code JRQ) and A508 Cl.3 (code JFL) were scrutinized for possible deviations of the postulated invariant MC shape and the MC validity for macroscopically inhomogeneous microstructure. Besides tensile and Charpy-V tests, MC tests were performed on Charpy-size three-point bend specimens in the unirradiated, neutron irradiated with fluences up to nearly 10^{20} n/cm^2 ($E > 1$ MeV) and recovery heat treated condition. Evaluation procedures include Master Curve reference temperature T_0 determination according to ASTM E1921-05 as well as additional analysis methods such as SINTAP, multi-modal MC method (MML) and the Unified Curve (UC). Integrity assessment according to ASME Code Cases N-629 and N-631 has been applied. It is shown that the standard MC concept provides a precise description of the fracture toughness for all conditions, even exceptionally well for the highly irradiated state. No MC shape change could be observed, whereas the UC concept indicates a significant influence of irradiation on the fracture toughness curves for the highly irradiated JRQ.

1. Introduction

The Master Curve (MC) method is gradually being incorporated into brittle fracture safety assessment procedures world-wide. While the VERLIFE methodology for WWER type reactor pressure vessel (RPV) integrity assessment (VERLIFE, 2003) directly uses the lower bound (5% fracture probability) curve, the ASME code cases N-629 (ASME, 2004) and N-631 (ASME, 1999) use the MC concept only indirectly. They now allow the use of a MC-based index temperature as an alternative to impact test- or drop-weight-test-based methods of adjusting the fracture toughness lower bound curve. The adoption of the MC concept in German KTA rules is under review. Some open issues still need solving, e.g. MC applicability to inhomogeneous and to highly neutron irradiated material and constraint effects of specimens with varying geometries and thicknesses. Therefore the German Federal Ministry of Economics and Technology (BMWi) has sponsored several research projects addressing these open topics (IWM, 2005; MPA, 2006; FZD, 2007; AREVA, 2007). In this paper the results of research project "Application of the Master Curve regarding characterization of the toughness of neutron irradiated reactor pressure vessel steels" (FZD, 2007) will be presented, which focused on highly neutron irradiated steels. Possible shape changes of the MC as found in highly embrittled Russian WWER-1000 RPV steel (Margolin et al., 2002) will be scrutinized for two RPV steels, ASTM A533B Cl.1 (code JRQ) and ASTM A508 Cl.3 (code JFL). Both RPV steels were investigated world-wide in different IAEA coordinated research projects (IAEA, 2001).

2. Irradiation damage

During the operation of a nuclear power plant RPV steels are subjected to intense radiation, primarily fast neutron irradiation. As a result complex changes in the microstructure take place, which are usually referred to as radiation damage. Background information can be found e.g. in Alekseenko (1997) and Odette and Lucas (1998). In summary, several irradiation effects on the microstructure have been identified. Direct matrix damage occurs due to elastic collision of fast neutrons with the metal atoms, which disturbs their ordered arrangement in the crystal lattice. Also, foreign atoms (He, H) may develop (Alekseenko, 1997). Moreover, voids and nanometer-sized copper-rich precipitates are formed (Ulbricht,

* Corresponding author. Tel.: +49 0 351 260 2766; fax: +49 0 351 260 2205.
E-mail addresses: c.zurbuchen@fzd.de (C. Zurbuchen), h.w.viehrig@fzd.de (H.-W. Viehrig), f.p.weiss@fzd.de (F.-P. Weiss).
[1] Tel.: +49 0 351 260 3246; fax: +49 0 351 260 2205.
[2] Tel.: +49 0 351 260 3480; fax: +49 0 351 260 3440.

0029-5493/$ – see front matter © 2009 Elsevier B.V. All rights reserved.
doi:10.1016/j.nucengdes.2009.03.008

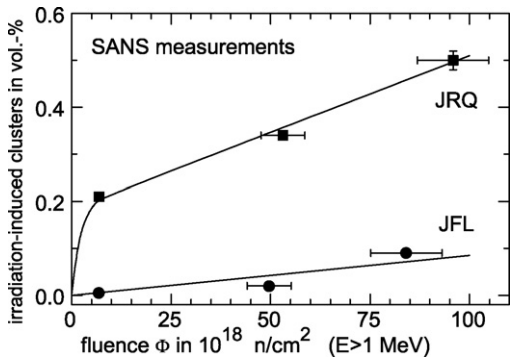

Fig. 1. Irradiation-induced cluster formation (Ulbricht et al., 2005).

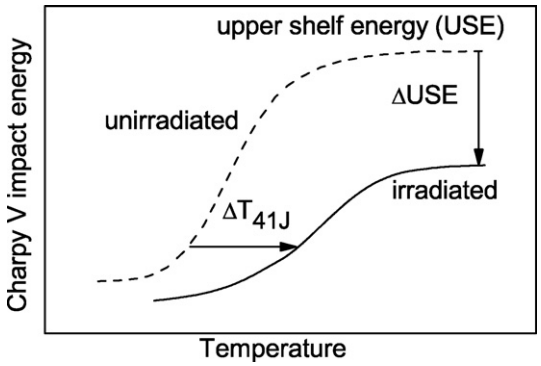

Fig. 2. Temperature dependence of the impact toughness.

2006) as well as embrittling phosphorus-rich segregations, preferably at grain boundaries (Pareige et al., 2004). Fig. 1 shows the irradiation-induced cluster formation of predominantly Cu-rich precipitates in the investigated RPV steels determined by SANS measurements (Ulbricht et al., 2005).

Neutron irradiation is known to reduce toughness properties, while strength properties increase simultaneously. In Fig. 2 typical temperature-dependent Charpy-V impact energy curves are drawn schematically. Irradiation usually shifts the curves to higher temperatures, expressed e.g. in terms of transition temperature T_{41J}, while the upper shelf of absorbed energy corresponding to full shear fracture (USE) decreases.

3. Master Curve concept and modifications

The scatter of fracture toughness in the transition region of low-alloyed body centered cubic ("ferritic") RPV steels can be modelled with Weibull statistics. This approach, proposed by Wallin (1984, 1985) and implemented in Test Standard ASTM E1921-05 (ASTM, 2005), characterizes the fracture toughness K_{JC} of ferritic steels at the onset of cleavage cracking. It uses a concept of universal temperature dependence of fracture toughness in the transition region, the so-called "Master Curve". The Master Curve is defined as the median fracture toughness of a specimen, adjusted to a crack front length of 1 T = 1 in. The temperature dependence of the MC is described by Eq. (1):

$$K_{JC(med)1T} = 30 + 70 \cdot \exp[0.019(T - T_0)] \quad (1)$$

where T_0 is the reference fracture toughness transition temperature that corresponds to the temperature at which $K_{JC(med)1T} = 100\,\text{MPa}\sqrt{\text{m}}$.

This simple formula which describes the shape of the median Master Curve is assumed to be constant for all ferritic (bcc) steel types, fluence levels, annealing heat treatments etc.

For material that contains randomly distributed macroscopic inhomogeneities two analysis extensions have been developed, the structural integrity assessment procedure SINTAP (1999) and the multi-modal (MM) method (Wallin, 2004; Viehrig et al., 2006). SINTAP contains a lower tail modification of the MC analysis which enables conservative lower bound type fracture toughness estimates. In the MM approach the total dataset is presumed to be composed of several, up to infinitely many, subsets (populations). Each subset follows the MC distribution but has a different T_0. The combined distribution is fully defined by two parameters: the mean reference temperature of all populations T_m, and the standard deviation around the mean σ_{Tm} (Scibetta, 2007).

As a simple criterion to decide if a dataset may represent a significant inhomogeneous microstructure, Eq. (2) is solved:

$$\sigma_{Tm} > 2 \cdot \sigma \quad (2)$$

i.e. the steel is likely inhomogeneous if the standard deviation of the MM estimation is more than double the value of theoretical scatter σ of the T_0 estimate according to ASTM E1921.

The outcome of the analysis enables to identify whether the material is likely inhomogeneous. Because the MM approach contains more parameters than the standard MC more specimens should be tested. Therefore, the dataset should satisfy the condition in Eq. (3), which is about double the number of specimens needed for a valid T_0 according to the standard MC evaluation.

$$\sum_i r_i \cdot n_i \geq 2 \quad (3)$$

where r_i is the number of valid specimens within the i-th temperature range, $(T–T_0)$, and n_i is the specimen weighting factor for the same temperature range as shown in Table 3 in ASTM E1921 (Scibetta, 2007). There are no exact analytical expressions for the multi-modal median fracture toughness curve and the fractiles. They are calculated individually for each dataset and may deviate from the standard MC shape.

Similar to the MC concept the Unified Curve was proposed by Margolin et al. (2001, 2003) as an engineering solution of the Prometey probabilistic model (Margolin et al., 1998a, 1998b). Apart from the multi-modal MC extension, the Prometey model is the only model able to describe a possible shape change of the fracture toughness-temperature curve for highly embrittled material, as found for WWER-1000 steel (Margolin et al., 2002), Fig. 3. The "highly embrittled" WWER-1000 steel for which the MC shape shows a significant deviation from the data points with many outliers and for which the UC proves to predict the shape change at high embrittlement correctly, was in fact not embrittled by neutron irradiation but by a specific heat treatment. Moreover, no information about possible intercrystalline crack growth has been given in (Margolin et al., 2002). According to Margolin et al. (2003),

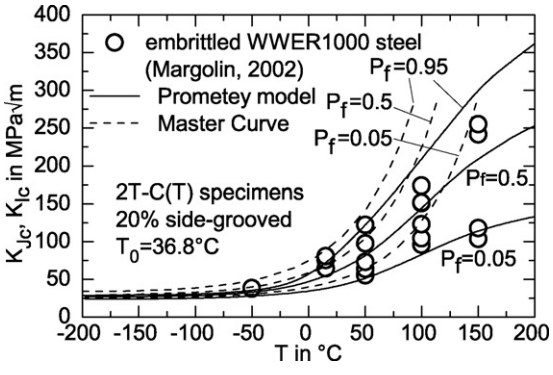

Fig. 3. UC and MC of "highly embrittled" WWER-1000 steel.

Table 1
Chemical composition (wt.%).

RPV steel	C	Si	Mn	Cr	Mo	Ni	P	Cu	S
JRQ	0.18	0.24	1.42	0.12	0.51	0.84	0.017	0.14	0.004
JFL	0.17	0.25	1.42	0.16	0.52	0.75	0.004	0.01	0.002

the MC concept can be considered a subcase of the Unified Curve concept.

The general Unified Curve $K_{JC}(T)$ dependence for any brittle fracture probability P_f and specimen thickness B is calculated similarly to the MC concept, Eq. (4). A minor difference exists regarding the choice of reference specimen thickness. According to ASTM E1921 $B_x = 1\,T = 25.4\,mm$ is to be used, while in the UC concept B equals 25 mm. In case of Charpy-size specimens this difference has a negligible effect: the UC choice results in a 0.4% higher $K_{JC(med)25mm}$ value compared with $K_{JC(med)1T}$.

$$K_{JC}(T)_{|P_f,B} = \left\{ K_{JC}^{shelf} - K_{min} + \Omega \cdot \left[1 + \tanh\left(\frac{T - 130}{105} \right) \right] \right\} \cdot \left(\frac{B_0}{B} \right)^{1/4} \cdot \left[\frac{\ln(1 - P_f)}{\ln(0.5)} \right]^{1/4} + K_{min} \quad (4)$$

where $K_{JC}^{shelf} = 26\,MPa\sqrt{m}$; $K_{min} = 20\,MPa\sqrt{m}$; Ω is a parameter that depends on the degree of brittleness, T is in units of °C, B_0 is the reference thickness of 25 mm and B is the specimen thickness in mm without consideration of side-grooves (Margolin et al., 2003).

Shape changes in the UC are accomplished by the hyperbolic tangent function, whose influence is governed by the value of Ω. With increasing embrittlement the value of Ω decreases, which promotes the tanh term, thereby resulting in a shallower $K_{JC}(T)$ curve compared with the MC. Examples of deviating shapes of MCs and UCs at various degrees of embrittlement can be found in Margolin et al. (2003, 2005). Ω itself is calculated iteratively according to Eq. (5) in which $K_{JC(i)}$ is either the valid experimental value obtained at test temperature T_i or, if censored according to ASTM E1921, its $K_{JC(limit)}$ substitute. Note that in both cases the data must be converted to $B_0 = 25$ mm before entry.

$$\sum_{i=1}^{N} \frac{\ln(2)(K_{JC(i)} - K_{min})^4 \left[1 + \tanh\left(\frac{T_i - 130}{105} \right) \right]}{\left\{ \Omega \left[1 + \tanh\left(\frac{T_i - 130}{105} \right) \right] - K_{min} + K_{JC}^{shelf} \right\}^5} - \sum_{i=1}^{N} \frac{\delta_i \left[1 + \tanh\left(\frac{T_i - 130}{105} \right) \right]}{\Omega \left[1 + \tanh\left(\frac{T_i - 130}{105} \right) \right] - K_{min} + K_{JC}^{shelf}} = 0 \quad (5)$$

where $K_{min} = 20\,MPa\sqrt{m}$; $K_{JC}^{shelf} = 26\,MPa\sqrt{m}$; N = number of specimen tested; $\delta_i = 1$ if the $K_{JC(i)}$ datum is valid or $\delta_i = 0$ if the datum is censored as defined in ASTM E1921.

Integrity assessment according to ASME Code Cases N-629 and N-631 permits the use of a MC-based reference temperature RT_{T0} Eq. (6) to adjust the ASME K_{IC} reference curve Eq. (7).

$$RT_{T0} = T_0 + 19.4\,K \quad (6)$$

$$K_{IC} = 36.5 + 22.783 \cdot \exp[0.036 \cdot (T - RT_{T0})] \quad (7)$$

where T is in °C and K_{IC} is in $MPa\sqrt{m}$, capped at $220\,MPa\sqrt{m}$.

4. Materials, specimens, irradiation conditions, experimental setup

Two Western type steels have been investigated. Chemical compositions are summarized in Table 1. The IAEA reference material JRQ (investigated block 3JRQ57, ASTM A533B Cl.1) has been extensively characterized since the 1980s (IAEA, 2001). It is well known for its high susceptibility to irradiation embrittlement because of unfavourable composition, notably medium Ni and high P and Cu contents, Table 1, and its manufacturing technology (rolled plates) resulting in an inhomogeneous microstructure. Micrographs of both steels can be found in FZD (2007). Networks of martensitic segregations were found (Müller, 2000). The prior austenite grain size is quite large, $27 \pm 14\,\mu m$ (Löwe, 2004). JFL (investigated block 1JFL11) denotes a forged ASTM A508 Cl.3 type steel comparable to the commercially used German RPV steel 22NiMoCr 3 7, containing very little P and Cu and exhibiting a more homogeneous, finely grained microstructure of $11 \pm 6\,\mu m$ (Löwe, 2004).

Table 2
Irradiation conditions.

RPV steel	Neutron fluence Φ in 10^{18} n/cm² ($E > 1$ MeV)	Maximum flux in 10^{12} n/(cm² s)
JRQ	7 (low)	0.14
	55 (medium)	3.01
	98 (high)	5.37
JFL	7 (low)	0.14
	51 (medium)	2.82
	87 (high)	4.74

All specimens were extracted from a region 1/4T to 3/4T wall thickness. The sectioning diagram and further experimental details are given in FZD (2007). For tensile tests sub-size specimens of 3 mm diameter and 15 mm gage length were machined (orientation T for JRQ and L for JFL). Besides standard Charpy-V specimens for impact tests (orientation T-L for JRQ and L-T for JFL), Charpy-size (10 mm × 10 mm × 55 mm) three-point bend specimens were fatigue-precracked to $a_0/W = 0.5$ and 20% side-grooved for MC tests (orientation T-L for JRQ and L-T for JFL).

All specimens sets were irradiated at the WWER-2 reactor of NPP Rheinsberg with fluences up to 10^{20} n/cm² ($E > 1$ MeV) at an average coolant temperature of 255 °C, cf. Table 2 for fluences. All given fluence values refer to a kinetic neutron energy level of $E > 1$ MeV. Depending on the distance of the irradiation channels to the reactor core the obtained fluences can be classified into three levels: "low" (ca. 7×10^{18} n/cm²), "medium" (ca. 55×10^{18}), and "high" (ca. 99×10^{18} n/cm²). For comparison, pressurized water reactors of latest design operating in accordance with German KTA rules should have their EOL fluence not larger than 3 to 10×10^{18} n/cm² for 40 years of operation (IAEA, 2001).

In order to study the effects of a recovery heat treatment, a set of irradiated specimens was annealed at 475 °C/100 h. To enhance the data pool new specimens were routinely reconstituted from broken Charpy-size specimen halves. Besides basic material characterization (microstructure, tensile properties), and Charpy-V tests according to EN 10045-1 (1990) the focus was set on the determination of reference temperatures T_0 according to ASTM E1921-05 (ASTM, 2005) by monotonically loading the specimen at a rate of $1.2\,MPa\sqrt{m}/s$ until cleavage instability occurs. Modified MC-based analysis methods such as SINTAP, multi-modal MC method (MM) and the Unified Curve were additionally applied.

In all evaluation procedures the following two formulae for the temperature dependence of 0.2% yield strength were used:

$$\sigma_{YS}(T) = 4 \times 10^{-8} T^4 - 2 \times 10^{-5} T^3 + 0.0036 T^2 - 0.543 T + 490.2 \quad (\sigma_{YS}\ \text{in MPa},\ T\ \text{in °C}) \quad (8)$$

for unirradiated JRQ according to IAEA (2001) and

$$\sigma_{YS}(T) = 0.0056 T^2 - 0.3269 T + 478.93 \quad R^2 = 0.984 \quad (9)$$

for unirradiated JFL (σ_{YS} in MPa, T in °C, $-135\,°C \le T \le +22\,°C$).

Irradiation hardening was considered by adding the respective $\Delta\sigma_{YS}$ shift values to these basic formulae.

Table 3
Mechanical-technological properties.

RPV steel	Φ in 10^{18} n/cm² (E > 1 MeV)	Tensile test		Charpy-V test	
		σ_{YS} MPa	UTS MPa	T_{41J} °C	USE °C
JRQ	0	484	618	−13	192
	7.3	689	798	111	144
	54.9	770	847	167	133
	98.2	843	904	209	111
JFL	0	470	614	−43	211
	6.5	534	666	−22	214
	51.2	587	706	9	196
	86.7	640	746	36	196

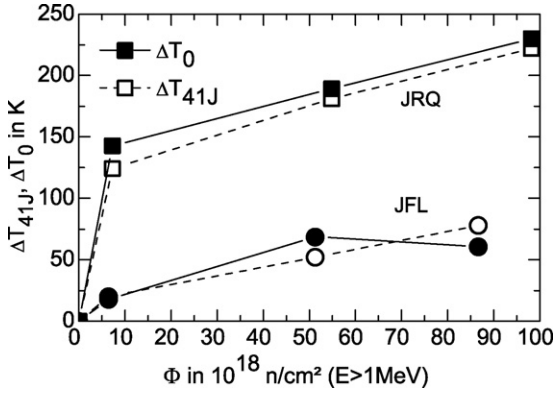

Fig. 4. Neutron irradiation-induced shifts of T_{41J} and T_0.

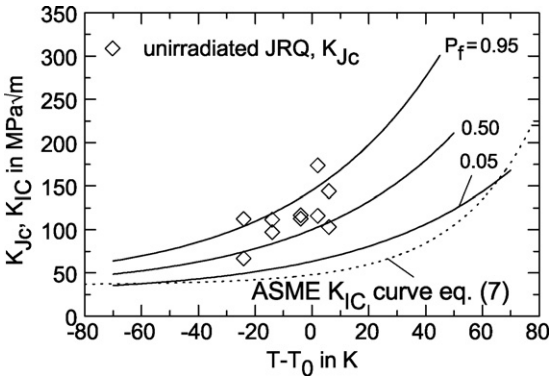

Fig. 5. MC results of unirradiated JRQ, adjusted to T–T_0.

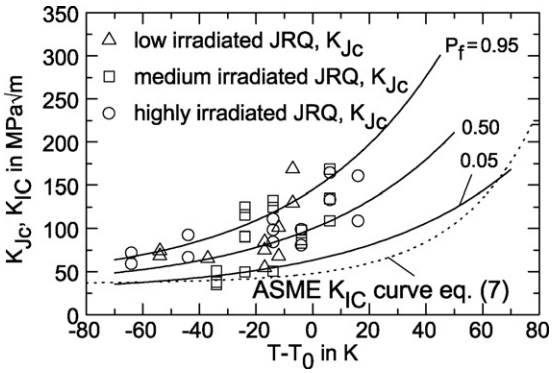

Fig. 6. MC results of irradiated JRQ, adjusted to T–T_0.

5. Results and discussion

Table 3 summarizes the results from tensile properties (yield strength σ_{YS} and ultimate tensile strength UTS) and Charpy-V parameters (T_{41J} transition temperature and upper shelf energy USE). Well-known irradiation effects can be found for both materials. Irradiation hardening is proven by increasing yield strength σ_{YS} and ultimate tensile strength UTS.

Embrittlement is expressed by increasing Charpy-V transition temperature T_{41J}, Table 3 and Fig. 4. However, the upper shelf energy USE does not follow such a clear trend, Table 3. In case of JRQ the upper shelf energy decreases to a great extent already at the low fluence, but it remains nearly unchanged for JFL for all irradiation levels up to nearly 100×10^{18} n/cm².

Results in Table 3 and Fig. 4 show that JRQ is the most irradiation sensitive steel whose properties tend to deteriorate significantly already at low fluence, while JFL is the quite insensitive. The same ranking can be observed in the Master Curve reference temperature T_0. Results of all MC tests are shown in Table 4 and Figs. 4–10.

Fig. 4 depicts the shift of T_0 with increasing fluence. Usually T_0 increases with irradiation (i.e. toughness decreases) but in Fig. 4 steel JFL poses an exception. Here T_0 decreases from medium to high fluence, which is in contradiction with the expected outcome of gradual irradiation-induced material degradation as seen in material properties from tensile tests or T_{41J} (Table 3). By an annealing heat treatment T_0 recovers to the values of the unirradiated state. As Table 4 shows this is true for both RPV steels alike and is independent of the reached fluence level.

Master Curve evaluation results are shown in Figs. 5, 6 and 7 for steel JRQ (in unirradiated; irradiated; and irradiated and annealed condition, respectively) and in Figs. 8, 9 and 10 for steel JFL (in unirradiated; irradiated; and irradiated and annealed condition, respectively). Beside the single K_{JC} test data adjusted to T–T_0 and

Table 4
K_{JC} evaluation according to MC, SINTAP, MM and UC.

RPV steel	Φ in 10^{18} n/cm² (E > 1 MeV)	Master Curve					Unified Curve (Margolin et al., 2001)	
		ASTM E1921-05			SINTAP	Multi-modal		
		Irradiated		Annealed	Irradiated	Irradiated	Irradiated	
		$\sum r_i n_i$	$T_0 \pm \sigma$ MPa	$T_0 \pm \sigma$ MPa	T_k^{SINTAP} °C	$T_m \pm \sigma_{Tm}$ °C	Ω	T_0^{UC} °C
JRQ	0	1.40	−65.6 ± 6	–	−65.6	–	1621	−67
	7.3	1.28	77.0 ± 6	–	87.3	(82 ± 17)	136	79
	54.9	2.57	123.6 ± 5	−73.2 ± 7	137.8	130 ± 25	72	133
	98.2	1.88	164.2 ± 5	−68.5 ± 7	164.2	–	50	186
JFL	0	2.38	−105.8 ± 5	–	−94.2	−104 ± 8	3286	−105
	6.5	1.12	−88.0 ± 7	−114.3 ± 7	−24.0	(−78 ± 22)	2472	−90
	51.2	3.17	−37.0 ± 4	−106.5 ± 6	−25.2	−27 ± 24	1000	−41
	86.7	3.35	−45.0 ± 4	−100.4 ± 6	−38.0	−40 ± 14	1098	−46

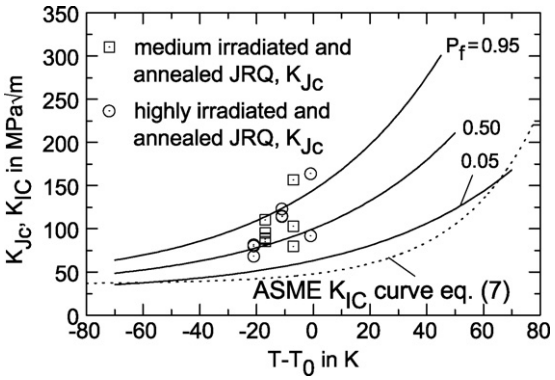

Fig. 7. MC results of irradiated and annealed JRQ, adjusted to T.

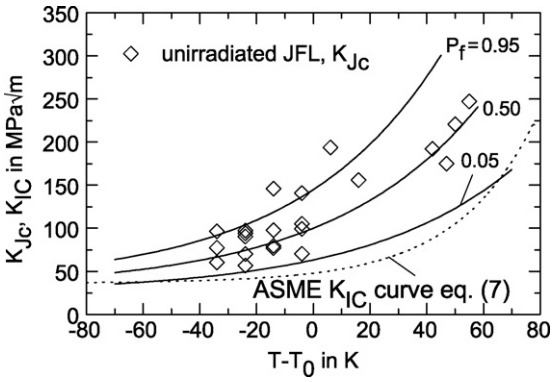

Fig. 8. MC results of unirradiated JFL, adjusted to T–T_0.

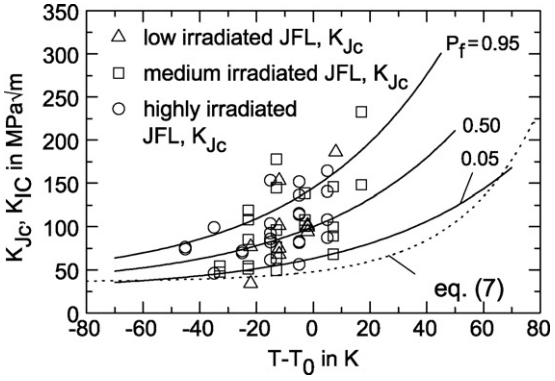

Fig. 9. MC results of irradiated JFL, adjusted to T–T_0.

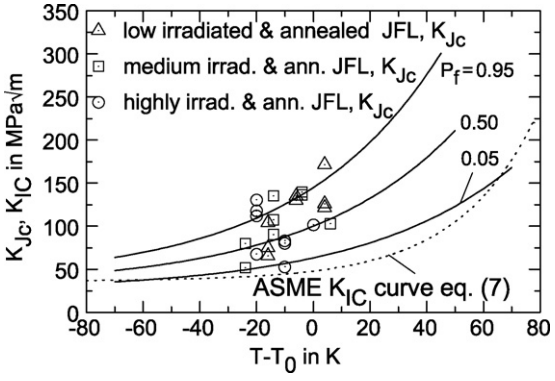

Fig. 10. MC results of irradiated and annealed JFL, adjusted to T–T_0.

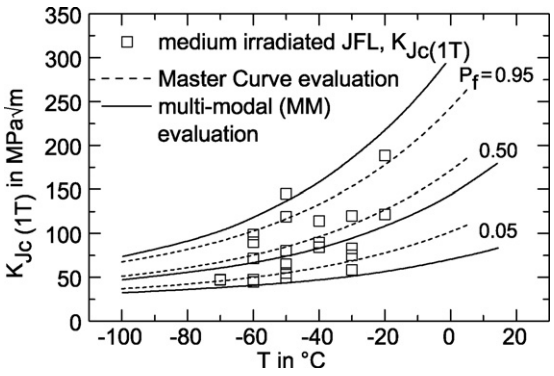

Fig. 11. MC and multi-modal evaluation of medium irradiated JFL.

the resulting 5%, 50% and 95% fracture probability Master Curves the ASME K_{IC}–RT_{T0} reference curve (Eqs. (6) and (7)) is drawn in each of the figures as a dotted line. Figs. 5–10 demonstrate that the 5% and 95% MCs envelope the data points well for each condition. Moreover, nearly all K_{JC} values lie above the ASME K_{IC} reference curve, i.e. only 2 out of 68 JRQ data points and 1 out of 99 JFL data points lie below it. Historically, the ASME K_{IC} curve was considered the absolute deterministic lower bound curve of fracture toughness below which no data points should lie. Our data confirms the findings in (Wallin, 1999) that the ASME K_{IC} reference curve in fact is just a deterministic lower bound curve to a specific subset of data, which represent a certain probability range. The ASME K_{IC} curve corresponds practically to the same degree of confidence as the 5% MC, thus permitting that few data points may lie below.

In order to investigate the above-mentioned unusual JFL behaviour, additional SINTAP and MM analysis methods were employed, Table 4 and Figs. 11 and 12. The SINTAP results T_k^{SINTAP} are by nature more conservative (higher) than standard MC T_0 estimates. Test results show that the SINTAP reference temperature T_k^{SINTAP} normally lies up to 15 K above T_0 (Table 4). The only case in which T_k^{SINTAP} and T_0 diverge significantly is for low irradiated JFL: T_0 is −88.3 °C and T_k^{SINTAP} is −24 °C. This deviance can be explained by the different SINTAP evaluation levels used to establish T_k^{SINTAP}. Aforementioned case is the only one for which the SINTAP evaluation algorithm does not favour the SINTAP step 2 estimate (which in this case equals −72.9 °C) but instead prefers the SINTAP step 3 estimate as the representative T_k^{SINTAP} value. The SINTAP step 3 reference temperature is even more conservative than SINTAP level 2, because it is derived from only one single K_{JC} value which represents the most brittle state, therefore resulting in such a comparatively high T_k^{SINTAP} value.

Table 4 and Figs. 11 and 12 show the MM results (solid lines) in comparison with standard Master Curves (dashed lines). Note

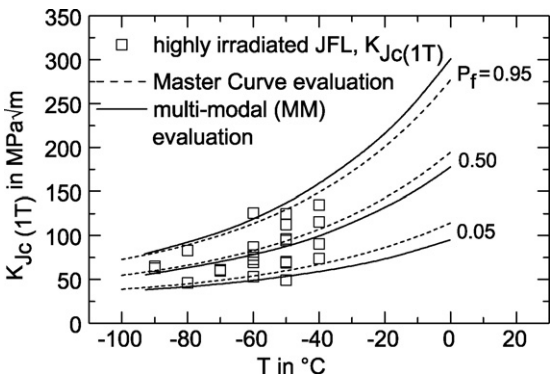

Fig. 12. MC and multi-modal evaluation of highly irradiated JFL.

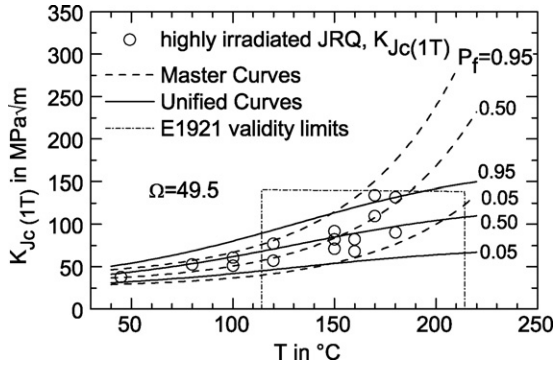

Fig. 13. MC and UC evaluation of highly irradiated JRQ.

the high standard deviation σ_m, which is associated with the low number of tested specimens. In order to reduce this uncertainty the specimen number requirement of Eq. (3) was introduced. MM results which do not satisfy Eq. (3) are parenthesized in Table 4. In both figures MM-based 5% and 95% failure probability curves are wider than their standard MC counterparts, thereby enveloping more data points. However, the MM analysis outcome follows the same trend as the standard MC evaluation: T_{0m} is higher in the medium irradiated JFL than in the highly irradiated state. SANS measurements of irradiation-induced defect density (Ulbricht, 2006) seem to offer an explanation for this unexpected result (Fig. 1). JFL shows little increment in matrix damage and Cu segregations once the medium fluence level was reached, presumably due to the material's very low Cu and P content which limits the ability to form embrittling Cu or P segregations. Taking the standard deviation σ into account, both T_0 values intersect at −41 °C, Table 4. Therefore the observed "decrease" of T_0 may as well be interpreted as a plateau formation of T_0 for fluences above 50×10^{18} n/cm^2 ($E > 1$ MeV). In contrast, all tensile and Charpy-V properties (aside from the upper shelf energy USE) continue to shift monotonically with the fluence increasing from medium to high levels.

Figs. 13 and 14 compare the results from MC and Unified Curve evaluation. The dashed lines in Figs. 13 and 14 depict the MC results of the highly irradiated states for JRQ and JFL, respectively. As can be seen, the MC describes the fracture toughness–temperature behaviour very well even at fluences as high as 100×10^{18} n/cm^2 ($E > 1$ MeV). This is true not only for RPV steel JFL but also for JRQ which exhibits a wide T_0 shift of about 230 K from the unirradiated state due to its high susceptibility to neutron embrittlement. For both RPV steels no significant MC shape change can be observed. In case of JFL, Fig. 14, more than 5% of the $K_{JC(1T)}$ values lie below the 5% failure probability Curve $K_{JC(0.05)1T}$. However, these probability curves are meaningful only for much larger datasets which contain dozens or hundreds of $K_{JC(1T)}$ values.

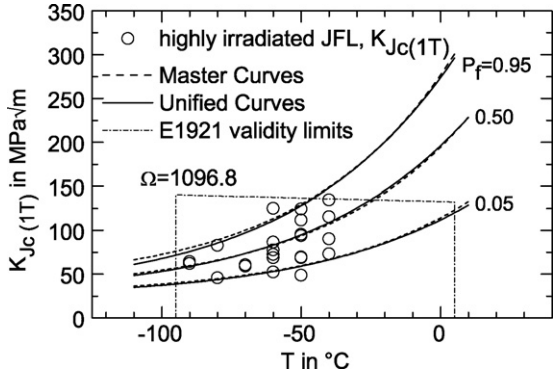

Fig. 14. MC and UC evaluation of highly irradiated JFL.

Table 4 and Figs. 13 and 14 combine the results of the Unified Curve (UC) and MC evaluation on the highly irradiated RPV steels (solid lines). T_0^{UC} (denoted T_{100} in Margolin's publications) is defined as the temperature at which $K_{JC(1T)}$ equals 100 MPa $\sqrt{m}$.

In case of steel JRQ, the Ω value is very low (49.6) which leads to very shallow UCs, Fig. 13. Compared with standard MC evaluation, the UC concept overpredicts the irradiation influence on the shape. T_0^{UC} is more conservative (higher) than T_0, Table 4.

In contrast, for highly irradiated steel JFL the UCs for 5%, 50% and 95% fracture probability coincide with the corresponding MCs (Fig. 14). 2 out of 23 $K_{JC(0.05)1T}$ values lie below the 5% MC. For JFL the shallowing influence of tangens hyperbolicus on the UCs is diminished by the high Ω value, which reflects the fact that JFL is much less susceptible to neutron embrittlement than JRQ. The MC reference temperature T_0 shifts only 61 K from the unirradiated to the highly irradiated state of JFL, Table 4.

As a mean to compare the goodness of fit of both approaches to the experimental data quantitatively, Margolin et al. (2003) and Margolin (2007) suggest the root mean square deviation, indexed with either MC or UC:

$$\delta_{MC,UC} = \sqrt{\frac{1}{L} \cdot \sum_{j=1}^{L} (K_{JC(med)j}^{pr} - K_{JC(med)j}^{exp})^2} \quad (10)$$

in which $K_{JC(med)j}^{pr}$ is the median value of K_{JC} at test temperature T_j predicted by the MC or UC and $K_{JC(med)j}^{exp}$ is the median value of K_{JC} at test temperature T_j determined by treatment of experimental data. The higher δ_{MC}/δ_{UC} the better the Unified Curve predicts $K_{JC}(T)$ compared with the Master Curve. Using $K_{JC(1T)}$ data in Eq. (10) yields the following results: For steel JRQ $\delta_{MC} = 15.19$ and $\delta_{UC} = 16.19$, thus $\delta_{MC}/\delta_{UC} = 0.89$ which means that the MC predicts the experimental data better than the UC (Fig. 13). Because the MC and the UC coincide in case of steel JFL (Fig. 14), it can be concluded that both describe the experimental $K_{JC(1T)}$ data equally well, which is reflected in a δ_{MC}/δ_{UC} ratio close to unity: $\delta_{MC} = 21.27$, $\delta_{UC} = 21.50$, thus $\delta_{MC}/\delta_{UC} = 0.99$.

The dot–dash lines in Figs. 13 and 14 are the MC validity window for Charpy-size specimens, i.e. ASTM E1921 rules that only data points tested at temperatures within $T_0 \pm 50$ K are permitted for T_0 calculation and all data points with K_{JC} above $K_{JC(limit)}$ are capped at this maximum value. In Fig. 13 it is demonstrated that data points are well described with the MC although they lie outside $T_0 \pm 50$ K range.

For MC shape investigations, Charpy-size (10 mm × 10 mm × 55 mm) specimens are not the best suited specimen geometries. Because of their low fracture toughness measuring capacity, K_{JC} values are usually censored as soon as the test temperature exceeds ca. $T_0 + 10$ K, and therefore they cannot cover the whole temperature range $T_0 \pm 50$ K as permitted by ASTM E1921. In order to explore possible MC shape changes above $T_0 + 10$ K with uncensored K_{JC} data, at least 0.5 T specimens or even better 1 T specimens are to be preferred because of their superior measuring capacity (Margolin, 2007).

6. Summary and conclusions

Two RPV steels A533B Cl.1 and A508 Cl.3 were scrutinized for possible deviations of the postulated invariant MC shape at neutron fluences up to 10^{20} n/cm^2 ($E > 1$ MeV) and the MC validity for macroscopically inhomogeneous microstructure.

MC tests were performed on Charpy-size three-point bend specimens in the unirradiated, neutron irradiated with fluences up to nearly 10^{20} n/cm^2 ($E > 1$ MeV) and recovery heat treated condition.

Evaluation procedures include Master Curve reference temperature T_0 determination according to ASTM E1921-05 as well as additional analysis methods such as SINTAP, multi-modal MC method (MML) and the Unified Curve (UC). The results have been compared with the ASME K_{IC} lower bound curve indexed with the MC-based RT_{T0} according to ASME Code Cases N-629 and N-631.

While tensile and Charpy-V material properties and also the MC reference temperature T_0 of RPV steels A533B Cl.1 change monotonically with the fluence increasing from 50×10^{18} to 100×10^{18} n/cm^2, RPV steel A508 Cl.3 poses an exception. From 50 to 100×10^{18} n/cm^2 T_0 decreases but taking the standard deviation into account this fact may be interpreted as a formation of a plateau. Most single K_{JC} data lie above the ASME K_{IC}–RT_{T0} reference curve. It could be shown that the standard MC concept provides a precise description of the experimental fracture toughness data for all conditions. It works exceptionally well for highly irradiated material. In contrast, the UC concept shows a significant influence of irradiation on the fracture toughness curves for the highly irradiated JRQ.

Acknowledgement

This study was sponsored by the German Federal Ministry of Economics and Technology (Reactor Safety Research Project Grant No. 150 1277).

Appendix A

Nomenclature

a_0	crack size (mm)
B	UC concept: reference specimen thickness: 25 mm
bcc	body centred cubic
B_0	gross specimen thickness, side-grooves not considered (mm)
B_x	MC concept: reference specimen thickness: 25.4 mm
$K_{JC(med)1T}$	median J-Integral based fracture toughness, adjusted to a crack front length of 1 T = 1 in. = 25.4 mm (MPa $\sqrt{m}$)
$K_{JC(med)25mm}$	UC concept: median fracture toughness, adjusted to a crack front length of 25 mm (MPa $\sqrt{m}$)
K_{JC}^{shelf}	UC concept: 26 MPa $\sqrt{m}$
K_{min}	MC and UC concept: 20 MPa $\sqrt{m}$
MC	Master Curve
MM	multi-modal Master Curve method
n_i	specimen weighting factor for the i-th temperature range, (T–T_0), Table 3 in ASTM E1921
P_f	fracture probability
PTS	pressurized thermal shock
r_i	number of valid specimens within the i-th temperature range, (T–T_0)
RT_{T0}	Master Curve based reference temperature
T	temperature (°C)
T	1 in. (25.4 mm)
T_0	MC reference temperature that corresponds to the temperature at which $K_{JC(med)1T}$ = 100 MPa $\sqrt{m}$ (°C)
T_0^{UC}	UC reference temperature that corresponds to the temperature at which $K_{JC(med)25mm}$ = 100 MPa $\sqrt{m}$ (denoted T_{100} in Margolin's publications) (°C)
T_{41J}	transition temperature measured at Charpy energy of 41 J (°C)
T_i	test temperature in UC concept (°C)
T_k^{SINTAP}	SINTAP reference temperature (°C)
T_m	multi-modal method: mean reference temperature of all populations
UC	Unified Curve
USE	upper shelf energy (J)
UTS	ultimate tensile strength (MPa)
W	specimen width (mm)

Greek symbols

δ_{MC}, δ_{UC}	root mean square deviation of experimental data from median MC/UC curves
$\Delta\sigma_{YS}$	shift value of σ_{YS} (MPa)
ΔT_0	shift of MC reference temperature
ΔT_{41J}	shift of Charpy-V transition temperature
Φ	neutron fluence in 10^{18} n/cm^2 (E > 1 MeV)
σ_{Tm}	multi-modal method: standard deviation around the mean
σ	theoretical scatter of the T_0 estimate according to ASTM E1921
σ_{YS}	0.2% yield strength (MPa)
Ω	Unified Curve concept: embrittlement parameter defining the Curve shape

References

Amaev, A.D., Gorynin, I.V., Nikolaev, V.A., Nikolaev, V.A., 1997. In: Alekseenko, N.N. (Ed.), Radiation Damage of Nuclear Power Plant Pressure Vessel Steels. American Nuclear Society, La Grange Park, Illinois.

AREVA, 2007. Final Report Grant Project No. 1501284: Determination of fracture mechanics values on irradiated specimens of German PWR Plants, AREVA NP GmbH, Erlangen.

ASME, 1999. ASME Code Case N-631: use of fracture toughness data to establish reference temperature for pressure retaining materials other than bolting for class 1 vessels. In: ASME (Ed.), ASME Boiler and Pressure Vessel Code Sec. III Division 1. ASME, New York.

ASME, 2004. ASME Code Case N-629: use of fracture toughness data to establish reference temperature for pressure retaining materials. In: ASME (Ed.), ASME Boiler and Pressure Vessel Code, Sect. XI: Rules for Inservice Inspection of Nuclear Power Plant Components Sec. XI Division 1. ASME, New York.

ASTM, 2005. ASTM Standard E1921, 2005, Standard test method for determination of reference temperature, T_0, for ferritic steels in the transition range. ASTM Intl., West Conshohocken, PA. Available from: <http://www.astm.org>.

EN 10045-1, 1990. Charpy impact test on metallic materials; Part 1: Test method. Beuth, Berlin.

FZD, 2007. Final Report Grant Project No. 1501277: Application of the Master Curve regarding characterization of the toughness of neutron irradiated reactor pressure vessel steels. Report No. FZD-476 2007, ISSN 1437-322X, FZD, Dresden.

IAEA, 2001. Reference Manual on the IAEA JRQ Correlation Monitor Steel for Irradiation Damage Studies, IAEA TECDOC-1230. IAEA, Vienna.

IWM, 2005. Final Report Grant Project No. 1501239: Critical investigation to the Master Curve concept for the application to German nuclear power plants. Report No. S8/2004, Fraunhofer-Institut für Werkstoffmechanik, Freiburg.

Löwe, A., 2004. Untersuchungen zur Bewertung von Reaktordruckbehälterstählen. TU Dresden, Faculty of Mechanical Engineering, Diploma thesis, Dresden.

Margolin, B.Z., Gulenko, A.G., Shvetsova, V.A., 1998a. Probabilistic model for fracture toughness prediction based on the new local fracture criteria. Int. J. Pressure Vessels Piping 75 (4), 307–320.

Margolin, B.Z., Gulenko, A.G., Shvetsova, V.A., 1998b. Improved probabilistic model for fracture toughness prediction for nuclear pressure vessel steels. Int. J. Pressure Vessels Piping 75 (12), 843–855.

Margolin, B.Z., Shvetsova, V.A., Gulenko, A.G., 2001. Towards fundamental understanding of the Master Curve. In: Symposium on RESQUE and REFEREE, 5–7 September 2001, Mol, Belgium.

Margolin, B.Z., Shvetsova, V.A., Gulenko, A.G., 2002. Comparison of the Master Curve and Russian approaches as applied to WWER RPV Steels. MASC Workshop "Use and Application of the Master Curve for Determining Fracture Toughness". VTT: 12–14 June 2002, Helsinki, Finland.

Margolin, B.Z., Gulenko, A.G., Nikolaev, V.A., Ryadkov, L.N., 2003. A new engineering method for prediction of the fracture toughness temperature dependence for RPV steels. Int. J. Pressure Vessels Piping 80 (12), 817–829.

Margolin, B.Z., Gulenko, A.G., Nikolaev, V.A., Ryadkov, L.N., 2005. Prediction of the dependence of K_{JC}(T) on neutron fluence for RPV steels on the basis of the Unified Curve concept. Int. J. Pressure Vessels Piping 82 (9), 679–686.

Margolin, B.Z., 2007. Experimental tests and analysis to compare different embrittlement assessment methodologies. In: TAREG meeting, 5–7 December 2007, Saint-Petersburg, Russia.

MPA, 2006. Final Report Grant Project No. 1501239: Critical examination of the master curve approach regarding application in German nuclear power plants. Report No. 8886 000 000. Materialprüfungsanstalt Universität Stuttgart, Stuttgart.

Müller, G., 2000. Untersuchungen zum Zusammenhang zwischen Seigerungen und Zähigkeitskennwerten des RDB-Stahles ASTM A533B cl.1 des Blockes 5JRQ22. FZR Report, FZ Rossendorf, FZR/FWSM-01/2000.

Odette, G.R., Lucas, G.E., 1998. Recent progress in understanding reactor pressure vessel steel embrittlement. Rad. Effects Defects Solids 144, 189–231.
Pareige, P., Radiguet, B., Kozodaev, M., Massoud, J.P., Zabusov, O., 2004. Atomic scale observation of the microstructure of a VVER 440 steel to understand properties of irradiated, annealed or re-irradiated materials. In: Technical Meeting on Irradiation Effects and Mitigation in RPV and Reactor Internals, 24–28 May 2004, Gus-Khrustalny, Russia.
Scibetta, 2007. Marc Scibetta, personal note.
SINTAP, 1999. SINTAP: Structural INTegrity Assessment Procedures for European Industry. SINTAP Procedure Final Version: November 1999.
Ulbricht, A., Böhmert, J., Viehrig, H.-W., 2005. Microstructural and mechanical characterization of radiation effects in model reactor pressure vessel steels. J. ASTM Int. 2 (10), 151–164.
Ulbricht, A., 2006. Untersuchungen an neutronenbestrahlten Reaktordruckbehälterstählen mit Neutronen-Kleinwinkelstreuung. PhD thesis, FZR-453, FZ Rossendorf, Dresden.
Viehrig, H.-W., Scibetta, M., Wallin, K., 2006. Application of advanced Master Curve approaches on WWER-440 reactor pressure vessel steels. Int. J. Pressure Vessels Piping 83 (8), 584–592.
Wallin, K., 1984. The scatter in K_{IC}-results. Eng. Fract. Mech. 19 (6), 1085–1093.
Wallin, K., 1985. The size effect in K_{Jc} results. Eng. Fract. Mech. 22 (1), 149–163.
Wallin, K., 1999. Statistical re-evaluation of the ASME K_{IC} and K_{IR} fracture toughness reference curves. Nucl. Eng. Des. 193 (3), 317–326.
Wallin, K., 2004. Overview of the Master Curve based techniques. ATHENA Workshop, 25–27 October 2004, Rome, Italy.